



Spectroscopic investigation of di- μ -hydroxo bridged platinum complexes
by John Raymond Marvin

A thesis submitted in partial fulfillment of the requirements for the degree of Doctor of Philosophy in Chemistry

Montana State University

© Copyright by John Raymond Marvin (1997)

Abstract:

When various Pt(II) complexes, coordinated in a *cis* fashion by certain monodentate sulfoxide and phosphane ligands, undergo hydrolysis, an extremely acidic (pH \sim 1.5-2.5) solution results. These hydrolysis reactions are accompanied by the formation of di- and occasionally tri-hydroxo bridged complexes which exist in equilibrium with the monomers at these low pH values. For the sulfoxide complexes, rapid scrambling of the sulfoxide ligands occurs between the two homodimeric forms in solution. The phosphane ligands, in contrast, appear to be considerably more substitutionally inert.

When monodentate sulfoxides are replaced by the bidentate sulfoxide ligand CH₃-S(O)-CH₂CH₂-S(O)-CH₃ (MSE), hydrolysis is followed by the formation of a complex mixture of products postulated to have a polymeric structure with the MSE ligand in a bridging role.

Heterodimeric structures were obtained when two different monomeric diaqua complexes containing neutral monodentate phosphane ligands were reacted in aqueous solution. Only the monomeric substitution product was observed when one of the monomers contained an anionic ligand (e.g. oxalate). A series of heterodimeric complexes containing the Pt(PMe₃)₂ fragment were systematically synthesized incorporating neutral nitrogen and sulfur donor ligands.

A novel network silver complex was obtained and characterized. This structure was initially formed as a result of the incomplete removal of Ag(I) ion used to assist in abstraction of chloride ion from the Pt(II) starting material. A crystal structure was acquired which shows the MSE ligand in a bridging mode.

Attempts to determine the acid dissociation constants of the monomeric diaqua complexes by potentiometric titration revealed a titration curve with only a single apparent inflection point, possibly indicating overlapping pK_a values. NMR titration of the trimethylphosphane system, plotting ¹H chemical shift vs. pH, revealed, two abrupt transitions which were associated with the pK_a's of the coordinated water ligands giving values of 6.5 and 9.6 for pK_{a1} and pK_{a2} respectively. The sum of these pK's was compared with the sum of the dimer formation (K_f) and dissociation (K_a) constants which had also been determined by NMR methods. K_f was found to be 2.701 ± 0.050 and K_d was found to be 22.008 ± 0.059 .

SPECTROSCOPIC INVESTIGATION OF
DI- μ -HYDROXO BRIDGED PLATINUM COMPLEXES

by

John Raymond Marvin

A thesis submitted in partial fulfillment
of the requirements for the degree

of

Doctor of Philosophy

in

Chemistry

MONTANA STATE UNIVERSITY-BOZEMAN
Bozeman, Montana

June 1997

D378
M36854

ii

APPROVAL

of a thesis submitted by

John Raymond Marvin

This thesis has been read by each member of the thesis committee and has been found to be satisfactory regarding content, English usage, format, citations, bibliographic style, and consistency, and is ready for submission to the College of Graduate Studies.

Edwin H. Abbott

Edwin H. Abbott 6/30/97
(Signature) Date

Approved for the Department of Chemistry

David M. Dooley

David M. Dooley 6/30/97
(Signature) Date

Approved for the College of Graduate Studies

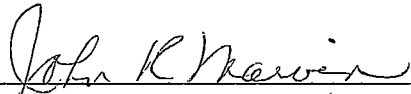
Robert L. Brown

Robert L. Brown 6/30/97
(Signature) Date

STATEMENT OF PERMISSION TO USE

In presenting this thesis in partial fulfillment of the requirements for a doctoral degree at Montana State University-Bozeman, I agree that the Library shall make it available to borrowers under the rules of the Library. I further agree that copying of this thesis is allowable only for scholarly purposes, consistent with "fair use" as prescribed in the U.S. Copyright Law. Requests for extensive copying or reproduction of this thesis should be referred to University Microfilms International, 300 North Zeeb Road, Ann Arbor, Michigan 48106, to whom I have granted "the exclusive right to reproduce and distribute my dissertation in and from microform along with the non-exclusive right to reproduce my abstract in any format in whole or in part."

Signature



Date

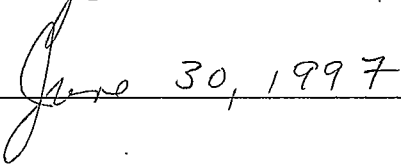


TABLE OF CONTENTS

	Page
LIST OF TABLES	vii
LIST OF FIGURES	xi
LIST OF EQUATIONS	xvii
ABSTRACT	xviii
 INTRODUCTION	 1
General Phenomenon of Metal Ion Hydrolysis	2
Statement of Objectives	8
Hydrolysis of 2 nd and 3 rd Row Platinum Group Metals	8
Practical Applications of the Research	12
Partially Oxidized and Mixed Valence Complexes	16
Oxidation of Pt(II) to Pt(IV)	18
Models for Homogenous Catalysis	23
Biologically Active Compounds	28
Structural Features and Proposed Mechanism of Formation of Di- μ -hydroxo Bridged Complexes	31
Homo- and Heterodimeric Pt(II) Sulfoxide Complexes	38
Monodentate Bis-sulfoxide Pt(II) Complexes	39
Bidentate Sulfur Donor Ligands	43
Monodentate Platinum(II) Phosphane Complexes	49
Ligands With Other Group 15 Donor Atoms	52
Reactions of Coordinated Ligands	51
Spectroscopy	55
Nuclear Magnetic Resonance Spectroscopy	55
 EXPERIMENTAL	 58
Instrumental Methods	58
Nuclear Magnetic Resonance Spectroscopy	58
Infrared Spectroscopy	61
Ultraviolet-Visible Spectroscopy	61
pH Measurements and Melting Point Determination	61

Preparation of Starting Complexes	62
<i>cis</i> -dichlorobis(dimethylsulfoxide)platinum (II)	62
Di- μ -hydroxobis(dimethylsulfoxide)platinum (II) nitrate	62
Dichloro(<i>trans</i> -1,2-diaminocyclohexane)platinum (II)	63
Di- μ -hydroxobis(<i>trans</i> -diaminocyclohexane) platinum (II) nitrate	63
Dichloroethylenediamineplatinum (II)	63
<i>Meso</i> -1,2-bis(methylsulfinyl)ethane	63
Silver(I)-trimethylphosphane Adduct	63
Silver(I) <i>meso</i> -1,2-bis(methylsulfinyl)ethane trifluoromethanesulfonate	64
Tetraaquaplatinum (II) perchlorate	64
<i>Cis</i> -dichlorobis(trimethylphosphane)platinum(II)	64
Dichlorobipyridilplatinum(II) and di- μ -hydroxo-bis-bipyridilplatinum(II) nitrate	65
Dichloro-1,2-bis(methylthio)ethaneplatinum(II)	65
Dichloro- α -1,2-bis(methylsulfinyl)ethaneplatinum(II)	65
Dichloro- β -1,2-bis(methylsulfinyl)ethaneplatinum(II)	65
Dichloro-1,2-bis(methylthio)ethanepalladium(II)	66
<i>Cis</i> -dichlorotetrakis(dimethylsulfoxide)ruthenium(II)	66
RESULTS AND DISCUSSION	67
Monodentate Platinum(II) Sulfoxide Complexes	67
Potentiometric Titration of $[\text{Pt}(\text{DMSO})_2(\text{OH}_2)_2] (\text{NO}_3)_2$	67
^{195}Pt NMR Titration of $[\text{Pt}(\text{DMSO})_2(\text{OH}_2)_2] (\text{NO}_3)_2$	71
Formation of Heterodimeric Monodentate Sulfoxide Complexes	76
Standard Addition of DESO	83
Monomeric Pt(II) and Pd(II) Complexes Containing Bidentate Sulfoxide Ligands	109
Hydrolysis Reactions of $\text{Pt}(\textit{meso}\text{-MSE})\text{Cl}_2$ (22)	113
Ag(I) Assisted Hydrolysis of <i>meso</i> - PtCl_2MSE (22)	114
Replacement of DMSO by <i>meso</i> -MSE	118
Reaction of $[\text{Pt}(\text{OH}_2)_4]^{2+}$ with <i>meso</i> -MSE	121
Bidentate Thioether Complexes of Pt(II)	128
Reaction of <i>cis</i> and <i>trans</i> $\text{Pt}(\text{Ox})_2(\text{OH}_2)_2$	135
Ruthenium Complexes Containing Monodentate Sulfur Ligands	143
A Brief Digression on Silver Chemistry	151
Oxidation of Sulfoxide Complexes	167
Mixed Valence Dimers	168
Platinum(II) Complexes With Phosphane Ligands	177
Formation of Pt(II)-Phosphane Mixed Ligand Dimers	183

Reaction of <i>cis</i> -Pt(PMe ₃) ₂ (OH ₂) ₂ (36) and <i>cis</i> -Pt(L) ₂ (OH ₂) ₂	183
Reaction of 36 With [Pt(bipy)(OH ₂) ₂] ²⁺	190
Reaction of 37 With [(dth)Pt(μ-OH) ₂ Pt(dth)] ²⁺	192
Reaction of 37 With [Pt(en)(OH ₂) ₂] ²⁺ (15).....	194
Thermodynamic Aspects of Dimer Formation.....	201
Determination of Dimer Formation Constant, K _f and Dissociation Constant, K _d	202
SUMMARY AND CONCLUSIONS.....	207
REFERENCES.....	209

LIST OF TABLES

Table	Page
1. pK_a values for some coordinated protic ligands	6
2. Partial list of platinum group metals currently being tested for anti-tumor properties.....	31
3. Platinum(II) complexes for which the pK_a 's of one or both of the coordinated waters has been determined.....	37
4. Phosphane ligand cone angles	51
5. Typical acquisition parameters for ^{195}Pt NMR spectra	59
6. Typical acquisition parameters for ^{31}P NMR spectra	59
7. Typical acquisition parameters for ^{13}C NMR spectra.....	60
8. ^{195}Pt chemical shifts for monodentate sulfoxide monomer and dimer complexes	77
9. Chemical shifts and coupling constants for all di- μ -hydroxo bridged binuclear complexes.....	80
10. Selected bond angles and distances for monodentate, di- μ -hydroxobridged dimeric platinum complexes	86
11. Crystallographic data for 18a and 18b	98
12. Atomic coordinates and equivalent isotropic displacement coefficients for <i>cis</i> -bis(dimethylsulfoxide)oxalatoplatinum(II) monohydrate (18a)	99
13. Atomic coordinates and equivalent isotropic displacement coefficients for <i>cis</i> -bis(dimethylsulfoxide)oxalatoplatinum(II) monohydrate (18b).....	99

LIST OF TABLES (continued)

14. Bond angles and standard deviations for <i>cis</i> -bis(dimethylsulfoxide)oxalatoplatinum(II) hydrate (18a).....	100
15. Anisotropic displacement coefficients for 18a	101
16. H-atom coordinates and isotropic displacement coefficients for 18a	101
17. Atomic coordinates and equivalent isotropic displacement coefficients for <i>cis</i> -bis(dimethylsulfoxide)oxalatoplatinum(II) hydrate (18b).....	102
18. Bond lengths for <i>cis</i> -bis(dimethylsulfoxide)oxalatoplatinum(II) hydrate (18b).....	103
19. Bond angles and standard deviations for <i>cis</i> -bis(dimethylsulfoxide)oxalatoplatinum(II) hydrate (18b).....	103
20. H-atom coordinates and isotropic displacement coefficients for 18b	104
21. Anisotropic displacement coefficients for 18b	105
22. ¹⁹⁵ Pt NMR data for oxalate and ethylenediamine complexes.....	106
23. NMR and IR data for monomeric halide complexes.....	113
24. Crystallographic data for <i>meso</i> -1,2-bis(methylsulfinyl) ethaneoxalatoplatinum(II) (31).....	138
25. Atomic coordinates and equivalent isotropic displacement coefficients for 31	139
26. Crystallographic data for <i>meso</i> -1,2-bis(methylsulfinyl) ethaneoxalatoplatinum(II) (31).....	139
27. Bond angles for <i>meso</i> -1,2-bis(methylsulfinyl) ethaneoxalatoplatinum(II).....	140
28. Anisotropic displacement coefficients for 31	141

LIST OF TABLES (continued)

29. H-atom coordinates and isotropic displacement coefficients for 31	141
30. Crystallographic data for <i>trans</i> -RuCl ₂ (<i>meso</i> -MSE) ₂ (33)	144
31. Atomic Coordinates and equivalent isotropic displacement coefficients for <i>trans</i> -RuCl ₂ (<i>meso</i> -MSE) ₂ (33)	146
32. Bond lengths for <i>trans</i> -RuCl ₂ (<i>meso</i> -MSE) ₂	147
33. Bond angles for <i>trans</i> -RuCl ₂ (<i>meso</i> -MSE) ₂	147
34. Anisotropic displacement coefficients for <i>trans</i> -RuCl ₂ (<i>meso</i> -MSE) ₂	149
35. H-atom coordinates and isotropic displacement coefficients for <i>trans</i> -RuCl ₂ (<i>meso</i> -MSE) ₂	150
36. Crystallographic data for silver(I) <i>meso</i> -1,2-bis(methylsulfinyl)ethane-trifluoromethanesulfonate (34)	155
37. Atomic Coordinates and equivalent isotropic displacement coefficients for 34	155
38. Bond Distances for 34	157
39. Bond angles for 34	159
40. Anisotropic displacement coefficients for 34	161
41. H-atom coordinates and isotropic displacement coefficients for 34	163
42. Crystallographic data for [Pt(Ox) ₂ (OH) ₂] ²⁻ [Pt(DMSO) ₂ (μ-OH)] ₂ ²⁺ • 3 H ₂ O (35)	173
43. Atomic coordinates and equivalent isotropic displacement coefficients for 35	173

LIST OF TABLES (continued)

44. Bond lengths for 35	174
45. Bond angles for 35	175
46. H-atom coordinates and isotropic displacement coefficients for 35	176
47. NMR data for trimethylphosphane heterodimeric complexes	198
48. Data used for calculation of dimer formation constant, K_f	203
49. Data used for calculation of dimer formation constant, K_d	205

LIST OF FIGURES

Figure	Page
1. Hydrolysis of metal cations	3
2. Plot of pK_a vs. electrostatic parameter (ξ) for some metal cations.....	4
3. Hydrolysis and polymerization of methyltrioxorhenium	7
4. Relationship between K_f , K_d , K_{a1} and K_{a2}	9
5. Equilibria between mono- and di-hydroxo bridged Cr(II), Rh(III) and Ir(III).....	11
6. Schematic Diagram of the Structure Directed Synthesis of a High Nuclearity Metal Complex.....	13
7. Bimetallic bridged structures formed by reaction of "precursor" and "target" complexes	15
8. General reaction scheme for the formation of high nuclearity pollymetallic complexes.....	16
9. Ligand field splitting for tetrahedral, octahedral and square planar d^8 coordination geometries.....	18
10. Oxidation of Pt(II) dimer with hydrogen peroxide.....	19
11. Pyrophosphito bridged Pt(III) dimer.....	21
12. Hypothetical structure of stacked dimer complex	22
13. Formation of di- μ -oxo bridged dimer	24
14. Synthetic applications of di- μ -oxo bridged dimers.....	25
15. Imide bridge substitution.....	26
16. Formation of mixed hydroxo-, peroxo bridged complexes	27
17. Fate of cisplatin under physiological conditions.....	29

LIST OF FIGURES (continued)

18. Formation of cross-links in double stranded DNA	29
19. Frontier orbital diagram illustrating the Hard-Soft Acid-Base theory	33
20. Partial molecular orbital diagram for metal-oxygen bonding	35
21. Hydrolysis and dimerization reaction for bulky Pt complexes.....	40
22. Resonance forms of dimethylsulfoxide.....	41
23. Two resonance forms of <i>meso</i> -1,2-bis(methylsulfinyl)ethane	43
24. Proposed scheme for HCl catalyzed transfer of oxygen to an organic sulfide	44
25. Introduction of chirality by transfer of oxygen from a sulfoxide to a symmetrical disulfide.....	46
26. Newman projection for <i>meso</i> -MSE	47
27. Sigma and pi bonding interactions in phosphane complexes.....	49
28. Illustration of cone angle for phosphane ligands	50
29. Formation and thermal decomposition of Di- μ -hydroxo bridged Pt(II) stibane dimers.....	53
30. Titration of a solution of 1 with 0.10 M NaOH	69
31. Dimerization scheme showing the liberation of two equivalents of H ₂ O and H ⁺	69
32. Species distribution as a function of pD for the <i>cis</i> -[Pt(dach)(OH ₂) ²⁺] system (pD = pH + 0.4).....	70
33. ¹⁹⁵ Pt NMR spectrum of an equilibrium mixture of <i>cis</i> -[Pt(DMSO)(OH ₂) ²⁺] and [Pt(DMSO) ₂ (μ -OH)] ₂ ²⁺	72
34. Plot of ¹⁹⁵ Pt chemical shift versus pH for a ~ 0.15 M solution of 1	73

LIST OF FIGURES (continued)

35. Species present in an equilibrium mixture of 5 and 6	78
36. ^{195}Pt NMR spectrum of an equilibrium mixture of equimolar 5 and 6	79
37. Diagrammatic illustration of the superposition of singlet and doublet spectra seen in J coupled ^{195}Pt NMR spectra.....	81
38. ^{195}Pt NMR of standard additions of 20, 40, 60, 80 and 325 mol% DESO to a solution of 5	84
39. Reaction scheme for the formation of the heterodimeric bridged complex containing both sulfur and nitrogen donor atoms.....	88
40. ^{195}Pt NMR spectrum for the reaction of 5 and 16 in the $\text{Pt}(\text{DMSO})_2$ region. pH= 6.8.....	90
41. ^{195}Pt NMR spectrum of the reaction of 2 with 1 equivalent ethylenediamine.....	91
42. Utilization of coulombic interaction to form a heterodimeric structure from one anionic and one cationic fragment.....	92
43. ^{195}Pt NMR spectrum of the reaction of 2 with an equilibrium mixture of $\text{Pt}(\text{oxalate})$ species; pH = 6.3.....	94
44. ORTEP plot for 18a	96
45. ORTEP plot for 18b	97
46. Packing diagram for 18a	107
47. Packing diagram for 18b	108
48. ^{13}C NMR spectrum of $\text{PtCl}_2(\text{meso-MSE})$ (22) in DMF.....	110
49. Ball and stick model of $\text{PtCl}_2(\text{meso-MSE})$ (22).....	112
50. Reaction scheme for the silver assisted hydrolysis of 22	114

LIST OF FIGURES (continued)

51. ^{195}Pt NMR spectrum for the reaction of $\text{PtCl}_2(\textit{meso}\text{-MSE})$ (22) with AgNO_3	116
52. ^{195}Pt NMR spectrum of the reaction of 22 and AgCF_3SO_3 at 60°C	117
53. ^{195}Pt NMR spectrum of the reaction of 2 with 1 equivalent of <i>meso</i> -MSE.....	120
54. Reaction of $[\text{Pt}(\text{OH}_2)_4]^{2+}$ with <i>meso</i> -MSE.....	121
55. ^{195}Pt NMR for the reaction of $[\text{Pt}(\text{OH}_2)]^{2+}$ with <i>meso</i> -MSE.....	123
56. Infrared spectrum of <i>meso</i> -MSE in the $\text{S}=\text{O}$ stretch region.....	124
57. Infrared spectrum of the reaction product of $\text{Pt}(\textit{meso}\text{-MSE})\text{Cl}_2$ with AgNO_3	125
58. Proposed structure for the hydrolysis product of 22	127
59. ^{195}Pt NMR spectrum of $\text{Pt}(\text{DTH})\text{Cl}_2$ (28) in DMF.....	130
60. ^{195}Pt NMR spectrum of the hydrolysis product of 28	131
61. The five invertomers of $[\text{Pt}(\text{DTH})(\mu\text{-OH})_2]^{2+}$ (29).....	132
62. ^{195}Pt NMR for an equilibrium mixture of 2 and 29	134
63. ORTEP plot of <i>meso</i> -1,2-bis(methylsulfinyl)ethane-oxalotitanium(II) (31).....	137
64. ORTEP diagram of <i>trans</i> -dichlorobis- <i>meso</i> -1,2-bis(methylsulfinyl) ethaneruthenium(II).....	145
65. ORTEP plot of $\{[\text{Pt}(\text{en})(\mu\text{-OH})_3]\text{Ag}(\text{NO}_3)_3\}^+$	152
66. ORTEP plot of silver(I) <i>meso</i> -1,2-bis(methylsulfinyl) ethane-trifluoromethanesulfonate (34).....	154

LIST OF FIGURES (continued)

67. Polyhedron diagram of 34	165
68. Packing diagram of 34	166
69. Proposed method for formation of mixed valence platinum dimers	169
70. ^{195}Pt NMR for the reaction of 1 and <i>trans</i> 30	171
71. ORTEP plot of $[\text{Pt}(\text{Ox})_2(\text{OH})_2]^{2-} [\text{Pt}(\text{DMSO})_2(\mu\text{-OH})_2]^{2+} \cdot 3 \text{H}_2\text{O}$	172
72. ^1H NMR titration of $[\text{Pt}(\text{PMe}_3)_2(\text{OH}_2)_2]^{2+}$	179
73. ^1H NMR spectra for the titration of $[\text{Pt}(\text{PMe}_3)_2(\text{OH}_2)_2]^{2+}$	180
74. Potentiometric titration of 36	182
75. Reaction scheme for the formation of $[\text{Pt}(\text{PMe}_3)_2(\mu\text{-OH})\text{Pt}(\textit{trans}\text{-dach})]^{2+}$ (39)	183
76. ^{31}P NMR spectrum of the hydrolysis product of <i>cis</i> - $\text{Pt}(\text{PMe}_3)_2\text{Cl}_2$	185
77. ^{31}P NMR of the reaction product of 37 and $[\text{Pt}(\textit{trans}\text{-dach})(\mu\text{-OH})_2]^{2+}$ (41) pH ~ 5.5	186
78. ^{195}Pt NMR of the reaction product of 37 and $[\text{Pt}(\textit{trans}\text{-dach})(\mu\text{-OH})_2]^{2+}$ (41)	188
79. 300 MHz ^{31}P NMR spectrum for $[\text{Pt}(\text{PMe}_3)_2(\mu\text{-OH})_2]^{2+}$ (37)	189
80. ^{31}P NMR for the reaction of 36 and $[\text{Pt}(\text{bipy})(\text{OH}_2)_2]^{2+}$	191
81. ^{31}P NMR for the reaction of 37 with $[\text{Pt}(\text{dth})(\mu\text{-OH})_2]^{2+}$	193
82. ^{31}P NMR for the reaction of 36 and $[\text{Pt}(\text{en})(\text{OH}_2)_2]^{2+}$ (15)	195
83. ^{195}Pt NMR spectrum in the region of the $\text{Pt}(\text{PMe}_3)_2$ fragment for the reaction of 36 and 15	196

LIST OF FIGURES (continued)

84. ^{195}Pt NMR spectrum in the region of the $\text{Pt}(\text{PMe}_3)_2$ fragment for the reaction of 36 and 15 ; pH.....	197
85. ^{195}Pt NMR spectrum for the reaction of 2 and 37	199
86. ^{31}P NMR spectrum for the reaction of 37 and $[\text{Pt}(\text{Et}_2\text{S})_2(\mu\text{-OH})]_2^{2+}$	200
87. ^{31}P NMR spectrum used in the determination of the dimer formation constant, K_f	204

LIST OF EQUATIONS

Equation	Page
1. Electrostatic parameter	4
2. Definition of Atomic Hardness	33
3. Shielding Constant of a Heavy Atom	55
4. Paramagnetic Term of Shielding Equation	56
5. Formation Constant Expression, K_f	203
6. Dissociation Constant Expression, K_d	205

ABSTRACT

When various Pt(II) complexes, coordinated in a *cis* fashion by certain monodentate sulfoxide and phosphane ligands, undergo hydrolysis, an extremely acidic (pH ~ 1.5-2.5) solution results. These hydrolysis reactions are accompanied by the formation of di- and occasionally tri-hydroxo bridged complexes which exist in equilibrium with the monomers at these low pH values. For the sulfoxide complexes, rapid scrambling of the sulfoxide ligands occurs between the two homodimeric forms in solution. The phosphane ligands, in contrast, appear to be considerably more substitutionally inert.

When monodentate sulfoxides are replaced by the bidentate sulfoxide ligand $\text{CH}_3\text{-S(O)-CH}_2\text{CH}_2\text{-S(O)-CH}_3$ (MSE), hydrolysis is followed by the formation of a complex mixture of products postulated to have a polymeric structure with the MSE ligand in a bridging role.

Heterodimeric structures were obtained when two different monomeric diaqua complexes containing neutral monodentate phosphane ligands were reacted in aqueous solution. Only the monomeric substitution product was observed when one of the monomers contained an anionic ligand (e.g. oxalate). A series of heterodimeric complexes containing the $\text{Pt}(\text{PMe}_3)_2$ fragment were systematically synthesized incorporating neutral nitrogen and sulfur donor ligands.

A novel network silver complex was obtained and characterized. This structure was initially formed as a result of the incomplete removal of Ag(I) ion used to assist in abstraction of chloride ion from the Pt(II) starting material. A crystal structure was acquired which shows the MSE ligand in a bridging mode.

Attempts to determine the acid dissociation constants of the monomeric diaqua complexes by potentiometric titration revealed a titration curve with only a single apparent inflection point, possibly indicating overlapping pK_a values. NMR titration of the trimethylphosphane system, plotting ^1H chemical shift vs. pH, revealed two abrupt transitions which were associated with the pK_a 's of the coordinated water ligands giving values of 6.5 and 9.6 for pK_{a1} and pK_{a2} respectively. The sum of these $\text{pK}'\text{s}$ was compared with the sum of the dimer formation (K_f) and dissociation (K_d) constants which had also been determined by NMR methods. K_f was found to be 2.701 ± 0.050 and K_d was found to be 22.008 ± 0.059 .

INTRODUCTION

The formation of larger and ever more complex structures from simpler precursors has long been one of the primary goals of the synthetic chemist. Until recently, success in this endeavor has belonged almost exclusively to the field of organic chemistry and, although the vast array of carbon chains and rings can hardly be expected to be matched by transition metals, a great deal of progress has been made in the last few years towards increasingly more complex and functional structures containing multiple metal atoms and metal-metal bonds. In the case of carbon, the enormous diversity of structures can be explained in part by the modest size of the carbon atom and its ability to form robust multiple bonds in small molecules. In the words of one eminent chemist, "Carbon does everything well and nothing to extreme" (1).

The chemistry of transition metals on the other hand is dominated by the availability of partially filled *d* orbitals. From the time of Werner at the beginning of the century up until the early 1960's, the properties of transition metal complexes were accounted for entirely in terms of individual metal atoms surrounded by a primary coordination sphere of ligands (2). It was not until the first experiments postulating the existence of a metal-metal bond were reported that the Wernerian concept of transition metal chemistry had to be modified to include a whole new class of

compounds, now referred to as metal cluster compounds. Clusters have since been defined as "a finite group of metal atoms that are held together mainly or at least to a significant extent, by bonds directly between metal atoms, even though some non-metal atoms may also be intimately associated with the cluster" (3). It should be emphasized that this definition specifically excludes complexes in which several metal atoms are held together exclusively by bridging ligands.

General Phenomenon of Metal Ion Hydrolysis

In the context of the preceding definition, the current work has focused on a specific class of di- μ -hydroxobridged compounds with a view towards using these species as building blocks for more complex structures. The creation of metal-metal bonds through oxidation of these complexes is expected to be a logical extension of this work but was of only secondary importance to understanding the fundamental chemistry surrounding the formation and reactivity of these dimers and higher oligomers. Because there were no specific "target" complexes in mind at the outset, each experiment was guided by the results of the previous one in an effort to find appropriate ligands with which to study the hydrolysis and polymerization reactions of the monomeric species.

It has long been known that metal ions undergo extensive and often complicated hydrolysis reactions in aqueous solution. Investigations into these species goes back to the pioneering work of N. Bjerrum (4) into the hydrolysis of chromium(III) and the introduction of the concept of "aquo acidity" introduced by Werner and Pfeiffer (5, 6). This process can be described as in Figure 1 which depicts the rapid and reversible hydrolysis of mononuclear species of a tri-positive metal ion such as Al(III) or Fe(III).

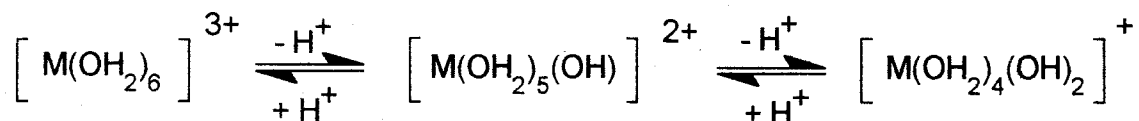


Figure 1. General reaction scheme for the hydrolysis of an aquated metal cation.

The relative strengths of aqua acids have been rationalized in terms of an ionic model which treats the metal ion as a hard sphere with radius r , and z units of positive charge (7). This model predicts that the acidity of the water in the primary coordination sphere of the metal cation should increase as the value of r decreases and as the charge on the metal increases, roughly paralleling the value of the electrostatic parameter given by Equation 1.

Equation 1 $\xi = z^2 / (r + d)$

where d is the diameter of the water molecule. This model works well for those metals from groups I and II of the periodic table that normally form ionic solids, but significant deviations are seen for many transition metals due to the departure from purely ionic interactions, as shown in Figure 2.

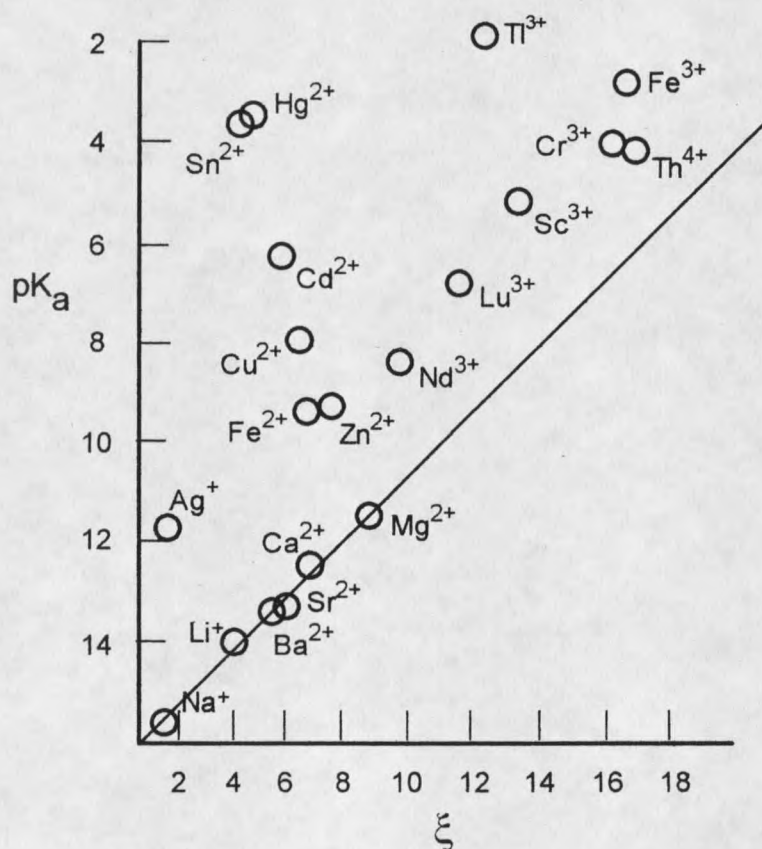


Figure 2. Plot of pK_a vs. electrostatic parameter (ξ) for some metal cations (7).

As the positive charge of the metal ion becomes delocalized over the entire complex, corresponding to a greater degree of covalent character, the proton of the coordinated water is repelled more strongly, resulting in a lower value of pK_a . Although it is probably not safe to extend this reasoning to other metals of the second and third row transition series, it is reasonable to expect that any factors which influence the charge distribution on a metal atom will affect the acidity of coordinated water molecules. Even for metals which do not adhere to this ionic model, the positive charge of the metal ion appears to stabilize the conjugate base of coordinated protic acids (8). The pK_a 's for some coordinated protic ligands are given in Table 1 (8, 9).

It has also been firmly established that many hydrolysis reactions are accompanied by polymerization, leading to complex and poorly characterized products. Well known examples include the formation of μ -hydroxo and μ -oxo iron(III) species at intermediate pH. After initial formation of a hydroxo bridge, the pK_a of the bridging hydroxide group is reduced considerably ($pK_a=6$) by coordination to not just one, but two metal atoms. These metal activated deprotonation reactions are not only important in inorganic systems but also have been postulated as important first steps in some metalloenzyme systems (8). Early studies often failed to recognize these polymerization reactions, resulting in erroneous conclusions concerning formation constants of hydrolysis products.

Table 1. pK_a values for some coordinated protic ligands for the reaction $[MLH]^n \rightleftharpoons [ML]^{n-1} + H^+$ (8, 9)

Metal	Metal Charge/Radius ^a	Ligand	pK_{a1}
-----		H ₂ O	14.0
Na ⁺	1.0	H ₂ O	negligible
Li ⁺	1.5	H ₂ O	13.7
Ca ²⁺	2.1	H ₂ O	13.4
Mg ²⁺	3.1	H ₂ O	11.4
Zn ²⁺	2.7	H ₂ O	10.0
Cu ²⁺	2.8	H ₂ O	10.7
Al ³⁺	6.7	H ₂ O	5.0
Cr ³⁺	4.8	H ₂ O	4.0
Fe ³⁺	4.7	H ₂ O	2.7
-----		NH ₃	35.0
Cu ²⁺	2.8	NH ₃	30.7
Ni ²⁺	-----	NH ₃	32.2
Co ²⁺	-----	NH ₃	32.9

a) Relative to Na⁺ = 1

An elegant example of polymerization involving the formation of μ -oxo bridges has recently been demonstrated by Herrmann et al. (10). Figure 3 shows a simplified reaction scheme for the spontaneous "self assembly" of methyltrioxorhenium monomers to form a three dimensional polymeric rhenium complex. This complex is reported to

have a metallic sheen similar to graphite and exhibits electrical conductivity in the solid state.

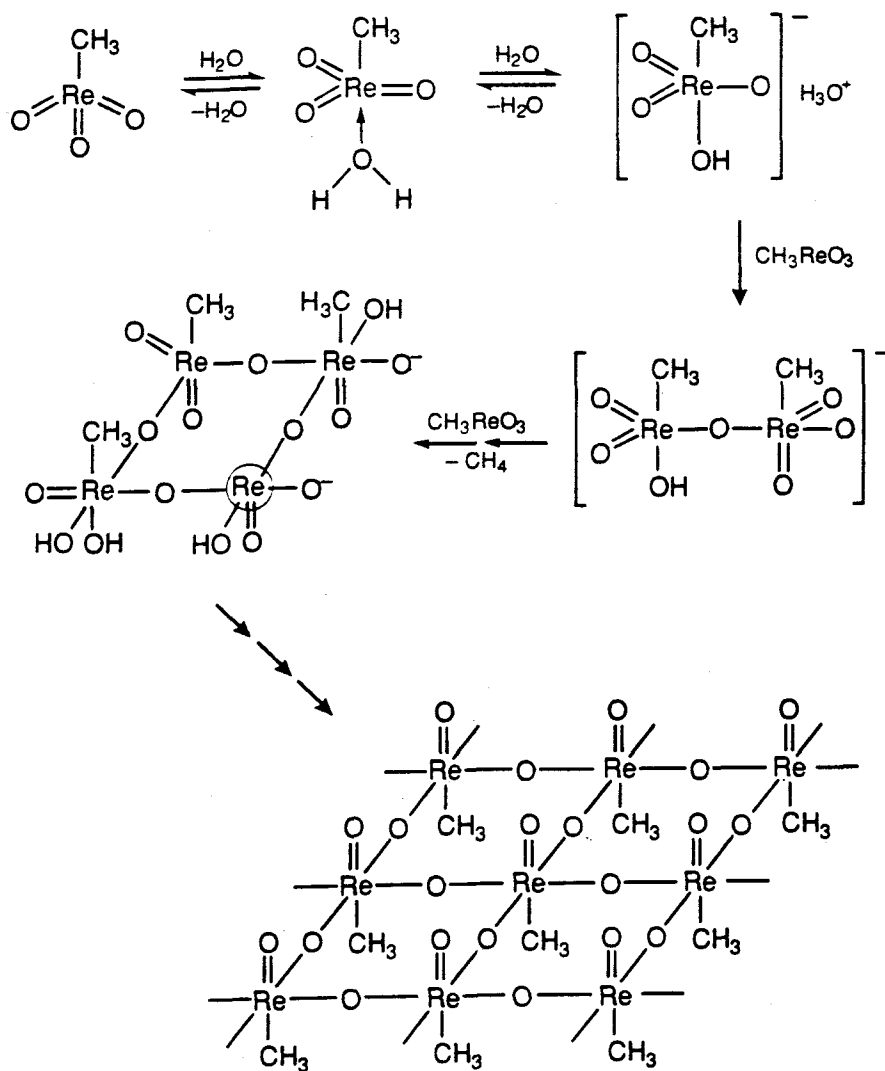


Figure 3. Hydrolysis and polymerization of methyltrioxorhenium (10).

Statement of Objectives

Hydrolysis of 2nd and 3rd Row Platinum Group Metals

The work presented here grew out of the observation that when Pt(II) is coordinated by certain sulfoxide or phosphane ligands, hydrolysis and deprotonation of the aqua ligands results in the formation of di- μ -hydroxo-bisplatinum(II) species, even under strongly acidic conditions (11, 12, 13). We have been interested in exploiting the marked tendency of these Pt(II) complexes to polymerize in acidic solution to develop methods for the systematic preparation of polymeric Pt(II) complexes and the oxidized Pt(IV) counterparts. The following therefore represents fundamental research into the formation of hydroxo bridged complexes and their equilibrium distribution as a function of pH. Of particular importance was determining the driving force behind these reactions, whether they were simply a result of the low pK_a 's of the coordinated waters in the monomeric hydrolysis products or whether there was some inherently greater thermodynamic stability conferred on the dimer as compared with the monomer. This last property is reflected in the values of the formation (K_f) and dissociation (K_d) constants shown in Figure 4 below.

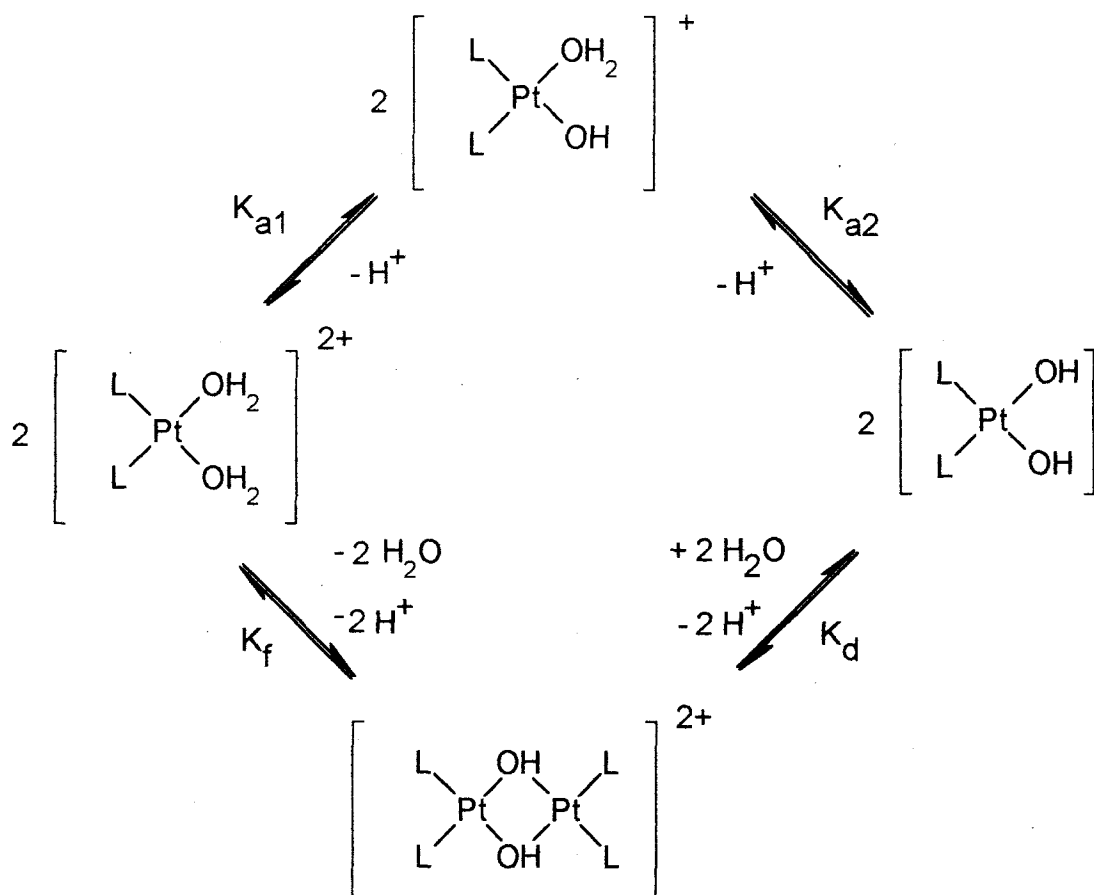


Figure 4. Relationship between K_f , K_d , K_{a1} and K_{a2} for dihydroxo bridged dimers.

As can be seen, the net reaction, starting with the *cis*-diaqua complex, releases two equivalents of water and two protons. Although the detailed mechanism is uncertain, the first step is thought to involve the deprotonation of one of the coordinated waters to form the aqua hydroxo complex. This singly charged cationic

species now has one highly nucleophilic ligand in hydroxide ion and one weakly nucleophilic leaving group in water. Dimer formation then simply requires two of these fragments to come together in the proper orientation, followed by release of the remaining water ligands. Other studies done on similar systems also provide strong evidence to suggest that the mono-deprotonated monomer is the reactive species in dimer formation at near neutral pH (15). At lower pH however, mechanistic studies indicate that the diaqua monomer also makes a substantial contribution to dimer formation (16). Any proposed mechanism for the formation of these dimeric species should be consistent with the established mechanisms for other square planar coordination complexes which normally involves the formation of a five coordinate intermediate (17).

It is useful to compare the mechanism for dimer formation in these four coordinate species with the fairly well established mechanism for hydroxo bridge formation in octahedral six coordinate complexes of other platinum group metals. These systems lend themselves to studies of this kind due in part to the much slower reaction times, with half-lives for the hydrolysis of dibridged Ir(III) amine and ammine complexes ranging from 60 to 9×10^6 seconds (18). Figure 5 shows the proposed reaction scheme for the equilibrium between mono- and dinuclear M(III) species (19). These reactions are thought to involve a well defined monohydroxo bridged intermediate shown in the figure. It has been postulated that a major stabilizing influence can be conferred on this intermediate by the hydrogen bonding interaction

shown between the singly coordinated water and hydroxo group of the aqua-hydroxo species.

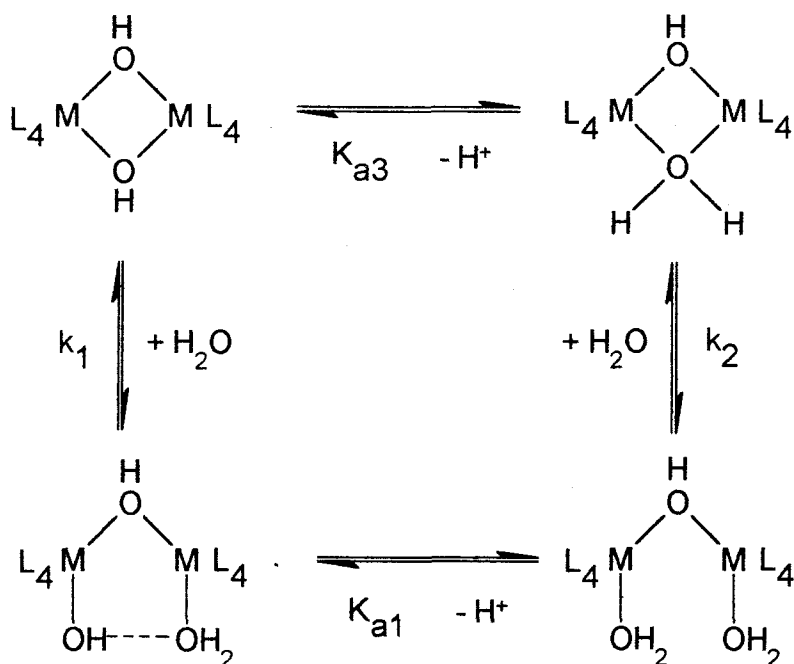


Figure 5. Reaction scheme for the equilibria between dinuclear mono- and dihydroxo-bridged species of Cr(II), Rh(III) and Ir(III). The dashed line indicates a hydrogen bonding interaction. (After Ref. 19)

The existence of this interaction has been confirmed in the solid state by X-ray diffraction data of the Ir(en) complex and is demonstrated in solution by examining the acid strength of mono- and dinuclear species (20). Mono-hydroxo bridged species of sufficient lifetime to be observed by NMR methods have also been postulated for several Pt(II) amine systems (21, 22, 23). Because the nonbonded distances between

the aqua and hydroxo ligands should be comparable in four coordinate square planar and six coordinate octahedral geometries, it is reasonable to expect that the same sort of stabilizing interaction may exist in square planar Pt(II) complexes.

Because these reactions are inherently pH dependent, the majority of our work was restricted to species which were at least partially water soluble. Many sulfoxide and several trialkylphosphane ligands form water soluble ionic complexes when coordinated to platinum and were therefore well suited to these investigations. Platinum was additionally convenient for this study due its favorable magnetic properties and intermediate reaction rates.

Practical Applications of the Research

Although the work presented here has concentrated on the basic synthesis and spectroscopic characterization of di- μ -hydroxo bridged complexes, fundamental research into polymerization reactions of this type are important for several reasons. The following briefly examines some of the possible practical applications of this work by discussing several synthetic strategies in which complex structures with very specific chemical and physical properties are "assembled" from two or more smaller fragments.

The systematic design and synthesis of "molecules with function" has recently emerged as an efficient route for more advanced materials applications involving transition metals.

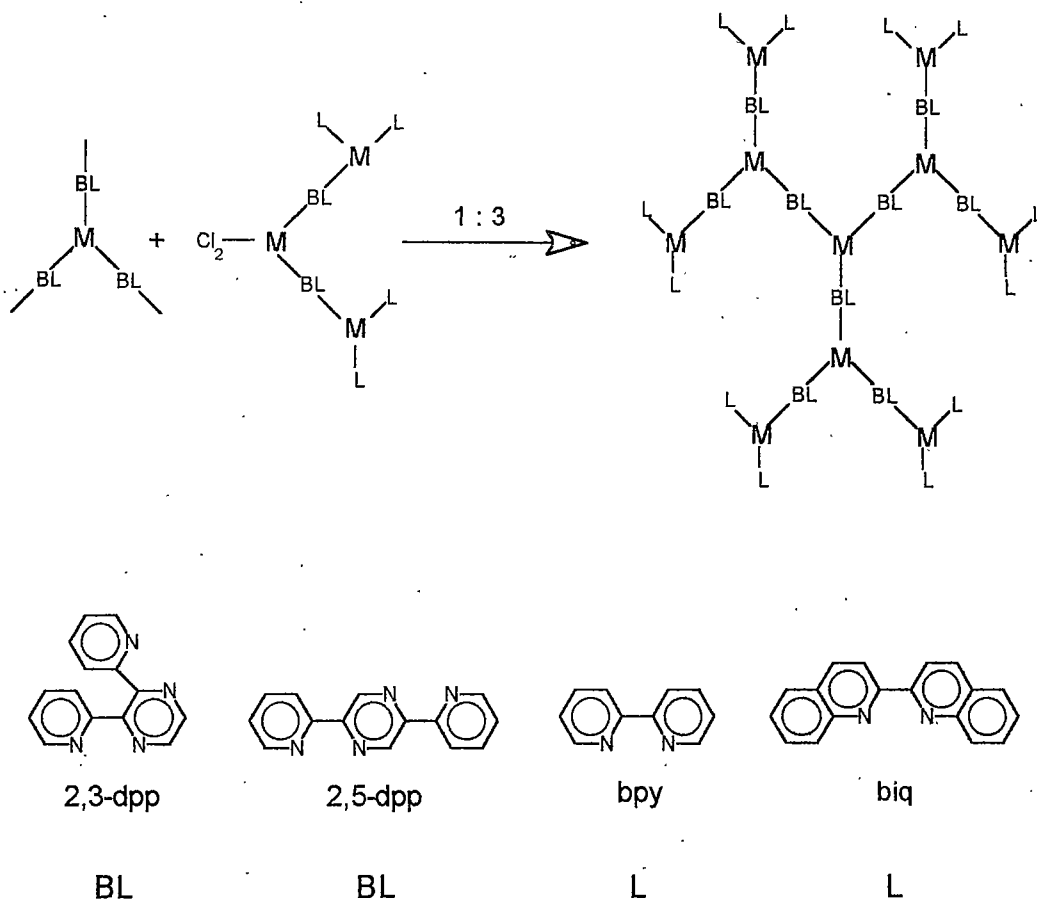


Figure 6: Schematic Diagram of the Structure Directed Synthesis of a High Nuclearity Metal Complex Using Complexes as Both "Metal" and "Ligand" (M = Ru or Os). The bridging (BL) and terminal (L) ligands used are also shown (24).

The systematic design and synthesis of "molecules with function" has recently emerged as an efficient route for more advanced materials applications involving transition metals.

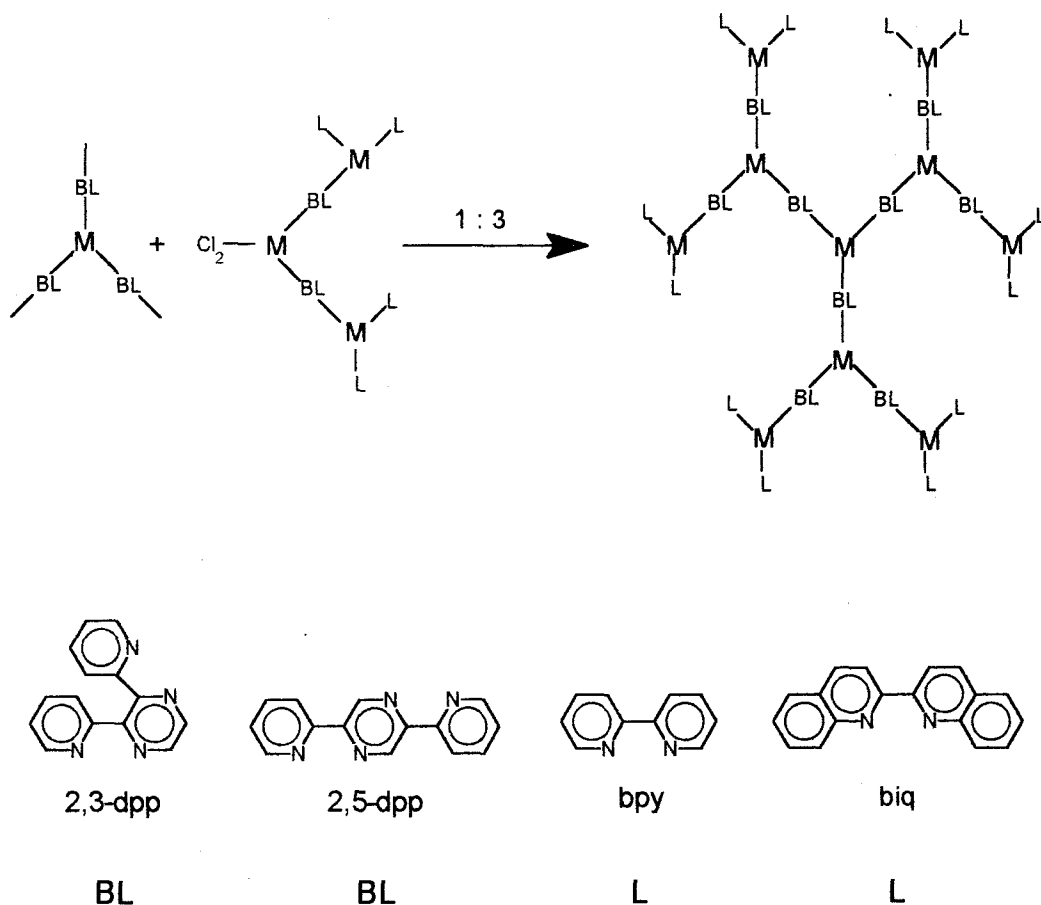


Figure 6: Schematic Diagram of the Structure Directed Synthesis of a High Nuclearity Metal Complex Using Complexes as Both "Metal" and "Ligand" (M = Ru or Os). The bridging (BL) and terminal (L) ligands used are also shown (24).

This strategy makes extensive use of multinuclear complexes as both "metal" and "ligand" and is exemplified by the synthesis of a host of closely related ruthenium complexes which can be systematically designed to possess a wide range of redox and luminescence properties (24). An example of this so called "structure directed synthesis" is shown in Figure 6. In the example shown, chloride provides a labile ligand on the metal atom. If this ligand is hydrolyzed by the addition of a silver salt, a free coordination site exists which is available to the "ligand" complexes. Only a few examples of this approach have been reported for platinum, including the homo- and heterodimeric complexes shown in Figure 7 (25). In this case, the synthesis of these complexes is accomplished by reacting a "precursor" Pt complex with a potentially bidentate amine ligand followed by reaction of the free functionality with a target complex (25). The potential of these complexes as potent second generation anti-tumor agents is discussed below.

A final example of the use of the structure directed approach applied to platinum group metals is seen in the elegant synthesis of bi- and tri-metallic complexes with the potential for applications in molecular circuitry. Figure 8 shows the synthetic use of alkynyl-bipyridine derivatives of Pt(II) as substrates for the addition of ruthenium and/or osmium fragments, resulting in a polymetallic species which shows unique electrical and luminescence properties (26). A brief discussion of molecular wires in the context of partially oxidized and mixed valence platinum complexes is given below.

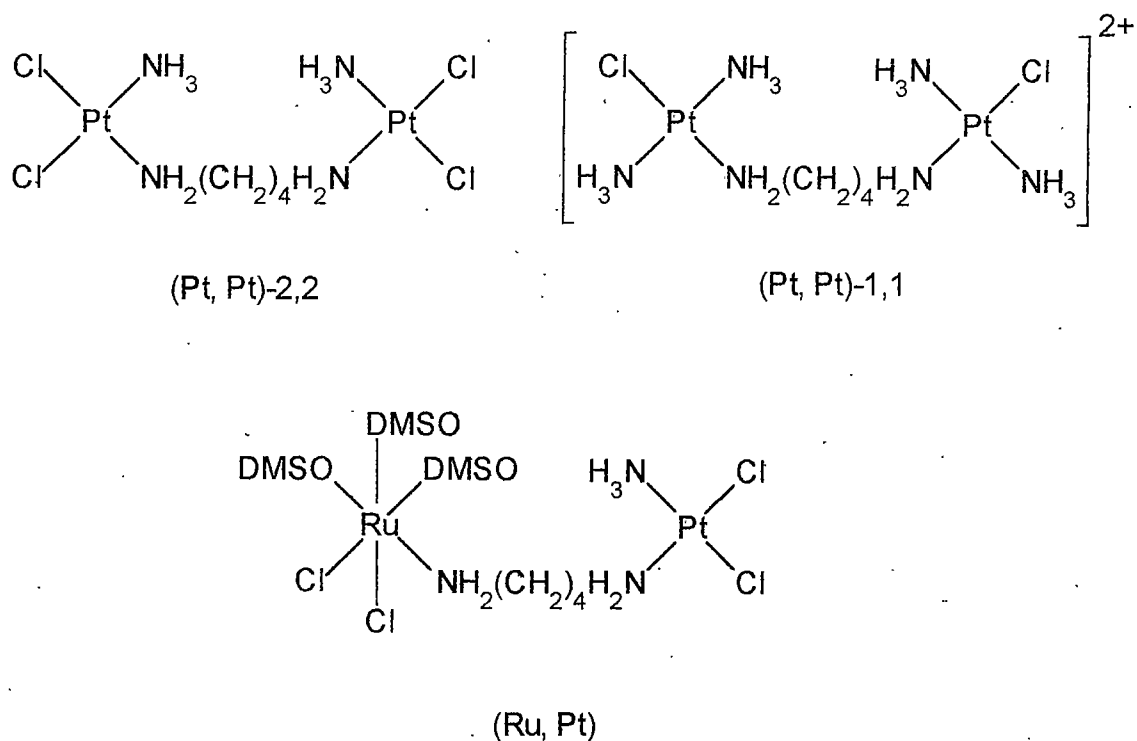


Figure 7. Bimetallic bridged structures formed by reaction of "precursor" and "target" complexes (25).

These examples serve to illustrate the tremendous potential of using polynuclear transition metal species as building blocks for structures with unique physical and chemical properties. It was one of the major goals of this research to determine whether di- μ -hydroxo bridged Pt complexes, with their inherent propensity toward polymer formation, and the availability of two free coordination sites at low pH, could be used in a similar fashion.

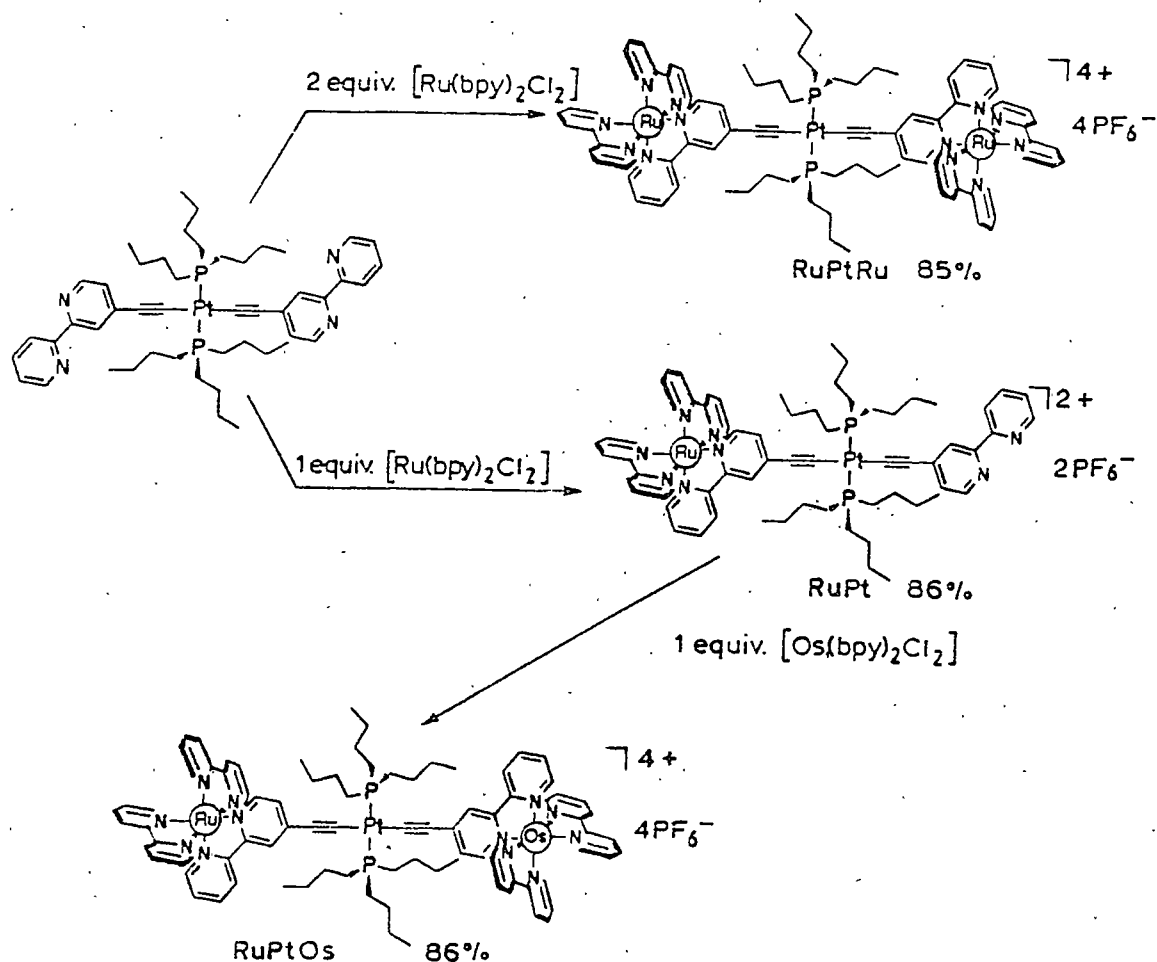


Figure 8. General reaction scheme for the formation of high nuclearity polymetallic complexes (26).

Partially Oxidized and Mixed Valence Complexes

The chemical properties of a transition metal complex can be dramatically altered by oxidation of the metal center. Until recently, the chemistry of platinum has been dominated by the two most stable oxidation states, +2 and +4. Platinum(II) almost invariably forms four coordinate square planar complexes typical of the other d^8

metals including Rh(I), Ir(I), Pd(II) and Au(III) (6). A few five coordinate Pt(II) species are known, including a proposed tri- μ -hydroxobridged dimer (27). These five coordinate species are of interest because of the structural information they may provide concerning the transition states for associative substitution reactions of square planar complexes. As mentioned previously, these reactions normally proceed through five coordinate trigonal bipyramidal intermediates (17). For first row d^8 metals such as Ni(II), tetrahedral complexes are formed with the weaker field ligands such as chloride and bromide, whereas square planar complexes are formed with strong field π donor ligands such as CN^- (28). The square planar configuration is favored over tetrahedral or octahedral geometry in this case due to the increased ligand field stabilization energy. This behavior can be explained using simple crystal field theory by appealing to the energy level diagram shown in Figure 9.

This diagram shows the ligand field splitting for tetrahedral, octahedral and square planar d^8 complexes as well as the tetragonal distortion representing the transition from octahedral to square planar geometry (29). In this diagram, the overall energy of the system can be lowered by pairing electrons in the d_{xy} orbital as the geometry moves from octahedral to square planar.

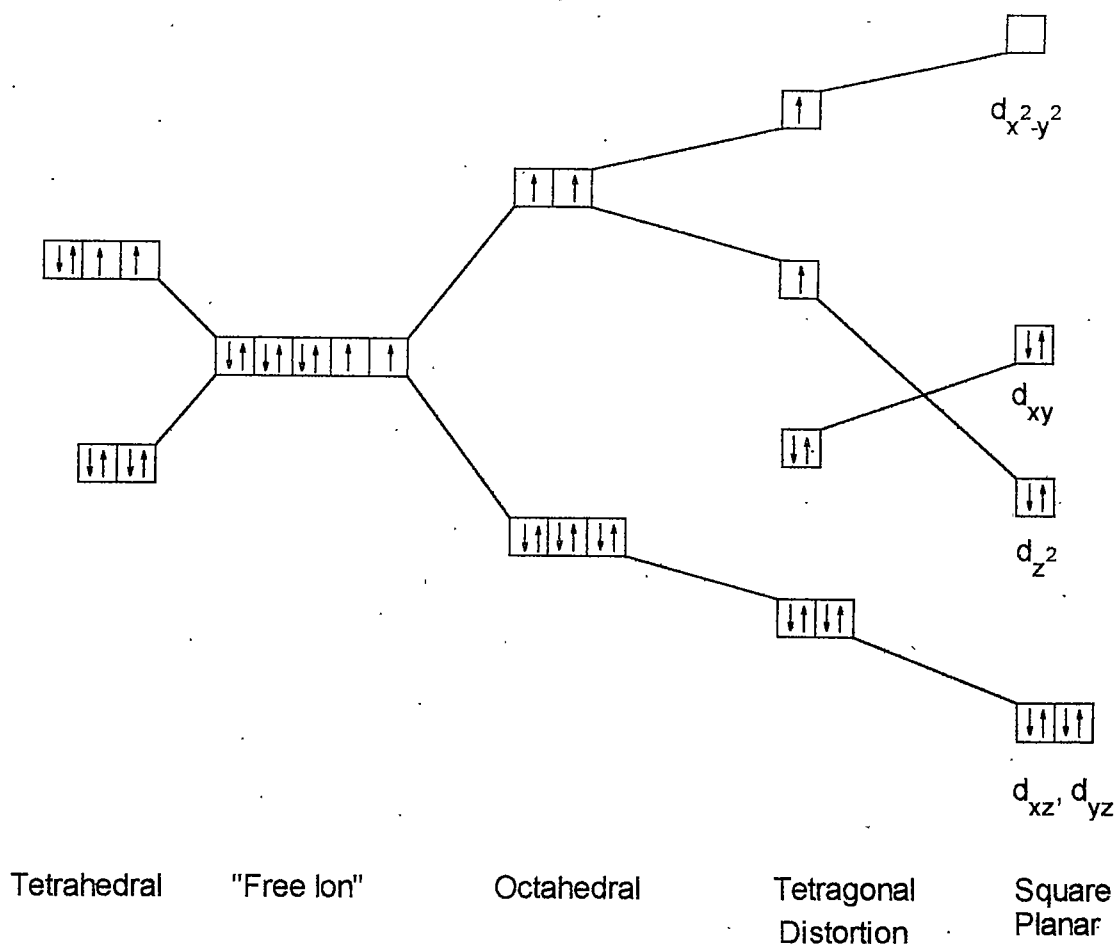


Figure 9. Ligand field splitting for hypothetical tetrahedral, octahedral and square planar d^8 coordination geometries (After Ref. 29).

Oxidation of Pt(II) to Pt(IV). Oxidation to the substitutionally inert Pt(IV) state can be accomplished by a variety of oxidizing agents. For the dimeric complexes being considered here, formation of the Pt(II) species followed by oxidation of one or both of the metal atoms could serve to lock the ligands in place, and would represent a significant step in being able to manipulate the reactivity of the dimer fragment. Only

one example of this type of reaction has been reported in the literature (30) (Figure 10). Hydrogen peroxide has also been shown to be effective at oxidizing *bis*-oxalato Pt(II) to the Pt(IV) *trans* dihydroxo complex. The mechanism for that reaction has been determined by ^{195}Pt NMR studies using isotopically labeled H_2O (31).

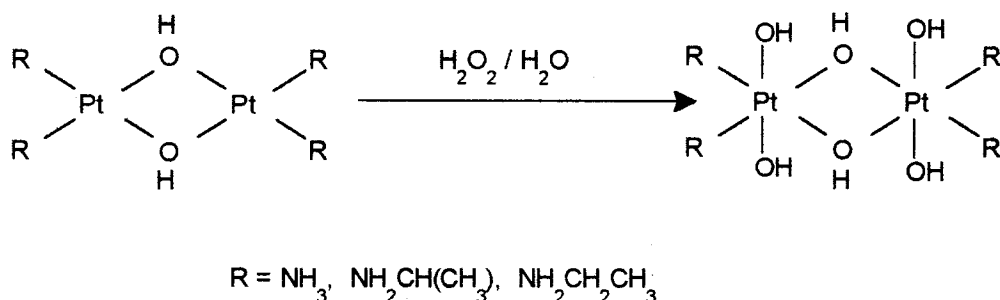


Figure 10. Oxidation of Pt(II) dimer with hydrogen peroxide (30).

Other oxidizing agents have also been successfully utilized for the oxidation of Pt(II) species, including cerium (IV), chlorine, bromine, monopersulfate ion and Pt(IV) (32, 33, 34, 35). Two electron oxidation with halogens normally produces the corresponding *trans* dihalo Pt(IV) species but also may result in halogen substitution on the more labile Pt(II) species if the reaction is carried out in aqueous solution. Because molecular chlorine disproportionates in aqueous solution, parallel oxidation by Cl_2 , HOCl , and OCl^- always occurs, the relative importance of each species being a

function of pH and concentration of free chloride. Details of reactions involving oxidation of monomeric and dimeric Pt(II) complexes pertinent to this investigation are discussed more fully in the Results and Discussion Section below.

The intermediate oxidation state of Pt(III) plays an important role in the formation of metal-metal bonded complexes and partially oxidized linear chain conductors. These octahedral d^7 complexes are substitutionally labile as well as being paramagnetic due to the unpaired electrons in the d_{xy} orbital. One of the most intensively studied classes of dimeric Pt(III) species is exemplified by the bridged pyrophosphito complex shown in Figure 11. In this structure, the metal p_z - p_z and d_z^2 - d_z^2 orbitals interact along the Pt-Pt axis to form a single metal-metal bond (36). A very important fundamental difference exists between the bridging geometry of this complex and the di- μ -hydroxo bridges discussed in this thesis. In the case of $[\text{Pt}_2(\mu\text{-PO}_4\text{H})_4]^{2-}$ the three atom span and the tetrahedral geometry around the interdonor oxygen atom create a face to face orientation of the PtO_4 units, thereby allowing the d_z^2 orbitals on each platinum atom to interact. Bonded Pt-Pt distances in these diplatinum (III,III) complexes range from 2.716 Å to 2.760 Å depending on the axial ligand, X (2). This range can be compared with the non-bonded Pt--Pt distance in di- μ -hydroxo bridged complexes which are all greater than 3 Å.

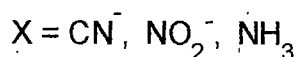
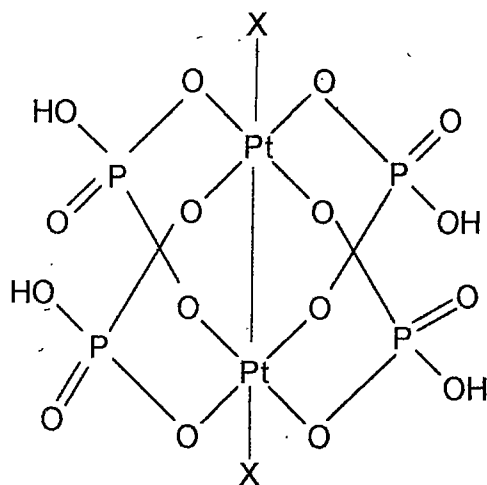


Figure 11. Pyrophospito bridged Pt(III) dimer (36).

It remains to be seen whether Pt-Pt bonds can be induced to form upon one electron oxidation of these dimeric species. The oxidation of mono- and dimeric Pt(II) sulfoxide and phosphane complexes is discussed more fully in the Results and Discussion section.

Although the individual d^7 metal centers are paramagnetic due to a single unpaired electron, polymer formation results in an overall diamagnetic " d^{14} " complex which can be studied by nuclear magnetic resonance spectroscopy. Chemical shifts have been reported for these complexes and appear to lie roughly midway between the

